Intrinsic effect of Mn doping in PZN–12%PT single crystals

Mouhamed Amin Hentati,[1,2] Mael Guennou,[1] Hichem Dammak,[1,a)] Hamadi Khemakhem,[2] and Mai Pham Thi[3]
[1]*Laboratoire Structures, Propriétés et Modélisation des Solides UMR 8580 CNRS, Ecole Centrale Paris, F-92295 Châtenay-Malabry, France*
[2]*Laboratoire des Matériaux Ferroélectriques, Faculté des Sciences de Sfax, Route Soukra Km 3,5, B.P.802, F-3018 Sfax, Tunisia*
[3]*Laboratoire Nanocomposites & Matériaux Hétérogènes, THALES Research & Technology, RD 128, F-91767 Palaiseau cedex, France*

(Received 22 November 2009; accepted 30 January 2010; published online xx xx xxxx)

In this work we study the influence of manganese doping on the electromechanical properties of PZN–12%PT single crystal. The full electromechanical tensor of doped PZN–12%PT in the tetragonal single domain state is determined by the resonance-antiresonance method. Doping leads to a decrease in the dielectric transverse permittivity ε_{11}^{T} and of the shear piezoelectric coefficient d_{15}. We show by dielectric constant ε_{33}^{T} measurements that the single domain state in doped crystal is stable in plates as thin as 90 μm, whereas it was unstable in plates thinner than 300 μm for the undoped crystals. This intrinsic effect is discussed by using a volume effect model based on the symmetry conforming principle of point defects. [Ren, Nature Mater. **3**, 91 (2004)]. Mn doping forces the stability of PZN–12%PT single domain state, which makes the doped crystal a most suitable candidate than the pure crystal for high frequency ultrasonic medical imaging probe. [doi:10.1063/1.3331817]

I. INTRODUCTION

High frequency ultrasonic imaging has many clinical applications because of its improved image resolution.[2] Its development has pushed the limits of ultrasonic imaging technology, giving diagnostic quality information about microscopic structures in living tissues. For high frequency devices, the thickness of the piezoelectric element must be less than 100 μm (Ref. 3) which has been a technological challenge for piezoelectric ceramics material. Therefore in recent years quite a bit of research has been directed to the development of single crystal piezoelectric materials like $[(1-x)Pb(Zn_{1/3}Nb_{2/3})O_3-xPbTiO_3]$ (PZN–x%PT). In the vicinity of the so-called morphotropic phase boundary (MPB) at x=9%, PZN–x%PT single crystals poled along a $[001]_C$ direction exhibit ultrahigh piezoelectric coefficients (d_{33} =2500 pC/N) and extremely large electromechanical coupling factor (k_{33}=92%) at room temperature.[4] Such excellent properties point to a potential revolution in electromechanical transduction used in ultrasound medical imaging probe.[5] Currently this application is limited by ferroelectric–ferroelectric transition present in compositions near the MPB which increase electromechanical properties temperature dependence, restricting then their temperature usage range. Recently, tetragonal PZN–12%PT single crystals have attracted more attention because of their high Curie temperature T_C ($\sim$190 °C) and no ferroelectric phase transition for $T<T_C$.[6] Although further away from the MBP, this material possesses reasonably high electromechanical coupling factor (k_{33} =86%) and piezoelectric coefficients (d_{33}=576 pC/N) while exhibiting a rather low longitudinal dielectric permittivity (ε_{33}^{T}=870).[7] With this properties PZN–12%PT is the best candidate to replace PZT ceramics used in ultrasonic medical imaging probe. However, for this composition, it was demonstrated that the single domain state of samples thinner than 300 μm is unstable,[8,9] while the relevant frequencies in ultrasonic imaging would require resonating plates thinner than 100 μm, making the practical realization of resonators a technological challenge.

Doping these compounds with acceptor cation like Mn^{2+} has been found to stabilize the domain structure.[10–13] This effect is generally attributed to a gradual pinning of domain walls by doping induced defects. These defects migrate to the domain boundary and consequently pin the domain walls. This effect can therefore be described as an "extrinsic effect" since it reduces the contributions to the electromechanical properties that are called "extrinsic," that is resulting from domain wall movements.[10,14] As a result, Mn doping reduces longitudinal piezoelectric coefficients (d_{33} and d_{31}) and electromechanical coupling factor (k_{33}, k_t, and k_{31}),[15–17] which lessen their capacity to be used in electromechanical transducer. Most of the previous studies on materials with multidomain structure attribute the stabilization of domain structure and the decrease in piezoelectric constants to the extrinsic effect.[15–17]

The influence of Mn doping on the intrinsic properties of the single crystals can be studied by examining the properties of doped and undoped crystals in their single domain state. Although the existence of a volume effect has been demonstrated in single domain $BaTiO_3$,[13] there are few reports that address this question in high performance PZN-PT or PMN-PT ($(1-x)PbMg_{1/3}Nb_{2/3}O_3-xPbTiO_3$) single crystals. A notable exception regarding PZN–12%PT single crystals is the work by Zhang *et al.*[18] who studies the influence of doping by various cations but does not give the full electromechanical tensor of the crystals.

In this work, we determine the full electromechanical

a)Electronic mail: hichem.dammak@ecp.fr.

TABLE I. Lattice parameters, at room temperature, of doped and nondoped PZN–12% PT single crystals poled along $[001]_C$ direction.

Lattice parameter	a (Å)	c (Å)
Mn–PZN–12%PT	4.019	4.0966
PZN–12%PT	4.025	4.0970

tensor of Mn-doped PZN–12%PT single crystals in its single domain state and we study the dependence of domain structure stability with the sample thickness. To explain the obtained results we further explored the microscopic origin of Mn doping on the basis of the universal defect symmetry principle.[1,19–21]

II. CRYSTAL GROWTH AND SAMPLE PREPARATION

Mn-doped PZN–12%PT single crystals (denoted Mn–PZN–12%PT) were grown using the conventional high-temperature flux method described elsewhere.[22,23] The concentration of Mn is of about 1 mol %. At room temperature, x-ray diffraction shows that Mn–PZN–12%PT single crystals have a tetragonal structure with lattice parameters a and c given in Table I. Crystals were oriented along $\langle 001\rangle_C$ pseudocubic directions and cut with different sizes and aspect ratios according to desired modes of resonance.[24] The Mn–PZN–12%PT samples were then polished and gold electrodes were sputtered on their relevant faces. Samples are then annealed at 700 K for 2 h to release stress induced by polishing. All samples were poled using the field cooling method[25] with a dc poling field of 1 kV/cm applied along a $[001]_C$ direction at 500 K with a cooling rate of 2 K/min. The paraelectric–ferroelectric transition temperature is slightly lower for doped crystals than for undoped crystals (457 K versus 472 K). The electromechanical properties were determined at room temperature by the resonance method[24] using an impedance analyzer (Agilent 4294A). The mechanical quality factor was computed using the relation $Q=f_r/(f_1-f_2)$, where f_r is the resonance frequency and f_1 and f_2 are the frequencies at 3 dB down to the maximum admittance.

III. RESULTS

A. Intrinsic effect of Mn doping on the electromechanical properties

The full electromechanical tensor of the single domain state 1T contains 11 independent coefficients. Table II shows our results on Mn–PZN–12%PT and those obtained recently on pure PZN–12%PT by Guennou *et al.*[26] The comparison shows that the elastic compliances can be considered unaffected by doping within the experimental uncertainties. Electromechanical coupling factor, piezoelectric coefficients (d_{33} and d_{31}), and dielectric permittivity (ε_{33}^T) show a slight increase upon doping. The most pronounced differences between doped and undoped crystals are exhibited by the transverse dielectric constant ε_{11}^T and the shear piezoelectric coefficient d_{15}: both decrease by approximately 40%. Last, the mechanical quality factors are considerably improved.

TABLE II. Electromechanical properties, at room temperature, of the tetragonal single domain state of Mn-doped and pure PZN–12%PT single crystals.

Properties	Mn–PZN–12%PT	PZN–12%PT[a]
ε_{11}^T	6000 ± 1000	$10\,000 \pm 500$
ε_{33}^T	870 ± 50	750 ± 50
$k_{31}(\%)$	$57{,}9 \pm 1{,}5$	$54{,}6 \pm 2$
k_{33}	$88{,}9 \pm 0{,}4$	$87{,}8 \pm 1$
k_t	$60{,}4 \pm 1$	60 ± 1
k_{15}	$51{,}6 \pm 4$	$49{,}7 \pm 3$
d_{31}(pm/V)	-230 ± 8	-207 ± 10
d_{33}	568 ± 30	541 ± 30
d_{15}	400 ± 80	653 ± 100
s_{11}^E(pm²/N)	$20{,}8 \pm 0{,}5$	$20{,}1 \pm 1$
s_{33}^E	$56{,}9 \pm 5$	$54{,}5 \pm 4$
s_{44}^E	$18{,}7 \pm 4$	$19{,}5 \pm 4$
s_{66}^E	$25{,}4 \pm 27$	$17{,}2 \pm 19$
s_{12}^E	$-5{,}5 \pm 11$	$-4{,}6 \pm 9$
s_{13}^E	$-17{,}7 \pm 6$	$-18{,}2 \pm 7$
Q_t	233 ± 50	50 ± 20
Q_{31}	880 ± 80	450 ± 100
Q_{33}	600 ± 60	440 ± 100

[a]Reference 26.

We note that the increase or the decrease due to Mn doping of a given electromechanical coefficient, ε_{ii}^T or $d_{i\alpha}$, depends on the direction of the ac-electric field. Indeed, all the piezoelectric and dielectric coefficients that are measured by application of the low ac-electric field along direction 3 increase slightly. On the other hand coefficients that are measured by application of electric field along direction 1 or 2 decreases. These results prove that Mn doping have an important intrinsic effect on the electromechanical properties that we should take into account.

B. Effect of Mn doping on the stability of single domain state

In pure PZN–12%PT, it has been shown previously that the tetragonal single domain state 1T was unstable in plates thinner than 300 μm.[8] This notably resulted in an increase in the dielectric constant for thin plates; while the longitudinal dielectric constant ε_{33}^T measured on bulk and thick samples amounts typically to 700, the dielectric constants measured on thinner plates increased gradually, reaching values as high as 2000 for 70 μm thick plates. This phenomenon, accompanied by a marked decrease in the overall electromechanical coefficient, is due to the emergence of domains lying in the plane of the plate.[8]

We carried out the same measurements on the doped single crystal and measured the dielectric constants for poled plates of various thicknesses down to 90 μm. Figure 1 shows the normalized longitudinal dielectric constant as a function of thickness for doped and undoped PZN–12%PT. For doped single crystal, the dielectric constant remains independent on the sample thickness at least until 90 μm. This result shows that Mn doping stabilizes the single domain state.

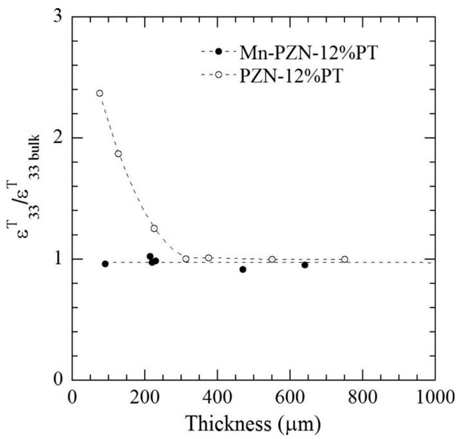

FIG. 1. Normalized longitudinal dielectric constant as a function of plate thickness. The value of $\varepsilon^T_{33\ \mathrm{bulk}}$ for single domain bulk samples is shown in Table II. Values of nondoped PZN–12%PT are those of Dammak *et al.* (Ref. 8).

IV. DISCUSSION

Our results show that doping has an influence on the properties of single domain states, which can only be an intrinsic effect. It is clear that the "domain walls pinning" model, described above in the introduction, based on "boundary effect" cannot explain this Mn doping behavior because domain walls are not present in the single domain state. The present experimental results can only be explained by a volume effect. The volume effect model proposed by Carl and Härdtl[27] and then by Lambeck and Jonker[13] seems most relevant. This model is based on a key assumption that there exist dipolar defects which follow spontaneous polarization P_S orientation after poling with the field cooling method. However this assumption does not has a microscopic explanation. Recent studies suggest that the volume effect arises from a symmetry conforming principle of point defects.[1,19,20,28] This latter model is widely used to explain reversible domain switching[21] and aging behaviors[28] in Mn-doped $BaTiO_3$ single crystals. In the following, the main ideas of this model are presented.

We first consider the valence and the chemical environment of Mn ions and their role in the crystal. It was shown in the case of Mn–PZN–4.5%PT (Refs. 16 and 29) that the largest fraction of Mn ions is Mn^{2+} ion (>90%) which replaces mostly titanium. The properties of the single crystal will thus be largely influenced by the presence of Mn^{2+} ions. The defect symmetry principle describes a relationship between crystal symmetry and the "symmetry" of statistical short-range-order distribution of point defects. To maintain charge neutrality, O^{2-} vacancies are necessarily produced. Consequently, the point defects in the crystal are Mn^{2+} dopants and O^{2-} vacancies. When samples are poled using the field cooling method with a high dc field applied along $[001]_C$ direction and a low cooling rate (as in our case), O^{2-} vacancies can migrate from O^{2-} site to an other. Within tetragonal structure, the first neighbor O^{2-} sites are not equivalent for the Mn^{2+} dopant. Due to a Coulomb attractive force between an effectively negative charged dopant and a positive charged vacancy, the probability of finding an oxygen vacancy in the nearest neighbor position of the Mn^{2+} dopant center is predicted to be highest along the crystallographic c axis. Then, the short-range-order distribution of defects tends to a tetragonal symmetry, which follows the tetragonal crystal symmetry.[19,20] The noncentrosymmetric distribution of charged defects forms a defect polarization P_D parallel to the direction of the spontaneous polarization P_S.

A key point in this model is the distinction between two types of dipole moments: ferroelectric dipole moment associated to cationic displacement, P_S, and dipole moments related to oxygen vacancies due to the polar tetragonal defect symmetry, P_D. This microscopic model agrees well with previous electron paramagnetic resonance experiments[30] and theoretical modeling[31,32] which suggest that defect dipoles tend to align along the spontaneous polarization P_S direction.

The stabilization of the single domain state in thin plates could be explained by the existence of defect dipole moments which provides forces that block the spontaneous polarization in its initial direction (Fig. 1). These forces, in the so-called "internal field," are responsible of the shifting of the polarization-electric field hysteresis loop along the E-axis.[13] In addition, these oriented defect dipoles should relax the structure along c axis and could be on the origin of the decrease in the measured tetragonal lattice parameter a perpendicular to the spontaneous polarization (Table I) which increase the tetragonality, i.e., the c/a ratio. This phenomenon is also observed in iron doped $PbTiO_3$.[33]

On the other hand, it was noticed that a perpendicular high electric field has to overcome an internal field produced by P_D before a microscopic dipole moment P_S switching can happen.[28] This makes spontaneous dipole moment switching in a poled doped single domain sample more difficult compared with the poled undoped sample. If we extrapolate this result to the low electric fields, we can conclude that the presence of defect dipole moment P_D makes P_S dipole moment rotation in a doped single domain sample more difficult compared with the undoped sample. This phenomena explains the decrease in dielectric transverse permittivity (ε^T_{11}) and of the shear piezoelectric coefficient (d_{15}) since these coefficients describe the capacity of polarization rotation under perpendicular low ac-field.[34,35]

V. CONCLUSION

In the present study we have determined the intrinsic effect of Mn doping on the stability of the single domain state and the electromechanical properties of tetragonal PZN–12%PT. Doping induces a decrease in the tetragonal lattice parameter, a, a stabilization of single domain state, a decrease in the dielectric transverse permittivity (ε^T_{11}) and the shear piezoelectric coefficient (d_{15}), and a moderate increment in piezoelectric coefficients (d_{33} and d_{31}) and dielectric permittivity (ε^T_{33}). Using a volume effect model based on the symmetry conforming principle of point defects leads to the presence of defect polarization, P_D, which relaxes the structure along c axis. These defects polarization should thus be on the origin of the decrease in the lattice parameter, a, and the reduction in the ability of polarization rotation, leading to a reduction in the transverse dielectric permittivity and the shear piezoelectric coefficient, and the stabilization of the single domain state down to a thickness of 90 μm. Finally the stability of longitudinal piezoelectric properties with doping represents an important result for applications especially in the high frequency ultrasonic medical imaging probe.

ACKNOWLEDGMENTS

The authors are grateful to French governments for financial support.

[1]X. Ren, Nature Mater. **3**, 91 (2004).
[2]K. K. Shung and M. J. Zipparo IEEE Eng. Med. Biol. Mag. **15**, 20 (1996).
[3]K. A. Snook, Z. Jian-Zhong, C. H. F. Alves, J. M. Cannata, C. Wo-Hsing, R. J. Meyer, Jr., T. A. Ritter,and K. K. Shung, IEEE Trans. Ultrson. Ferroelectr. Control **49**, 169 (2002).
[4]S. E. Park and T. R. Shrout, J. Appl. Phys. **82**, 1804 (1997).
[5]K. Uchino, *Piezoelectric Actuators and Ultrasonic Motors*, Kluwer Academic, Boston, 1996).
[6]D. La-Orauttapong, B. Noheda, Z.-G. Ye, P. M. Gehring, J. Toulouse, D. E. Cox, and G. Shirane, Phys. Rev. B **65**, 144101 (2002).
[7]S. J. Zhang, C. A. Randall, and T. R. Shrout, Solid State Commun. **131**, 41 (2004).
[8]H. Dammak, M. Guennou, C. Katchazo, M. P. Thi, F. Brochin, T. Delaunay, P. Gaucher, E. Le Clézio, and G. Feuillard, Proceedings of the 2006 15th IEEE ISAF, 2007, pp. 252–255.
[9]D. Y. Jeong and S. Zhang, J. Korean Phys. Soc. **44**, 1527 (2004).
[10]D. Damjanovic, Rep. Prog. Phys. **61**, 1267 (1998).
[11]G. Arlt and U. Robels, Integr. Ferroelectr. **3**, 343 (1993).
[12]D. A. Hall and M. M. Ben-Omran, J. Phys.: Condens. Matter **10**, 9129 (1998).
[13]G. H. Lambeck and P. V. Jonker, J. Phys. Chem. Solids **47**, 453 (1986).
[14]V. S. Postnikov, V. S. Pavlov, and S. K. Turkov, J. Phys. Chem. Solids **31**, 1785 (1970).
[15]Y. Chen, S. Hirose, D. Viehland, S. Takahashi, and K. Uchino, Jpn. J. Appl. Phys., Part 1 **39**, 4843 (2000).
[16]D. Kobor, L. Lebrun, G. Sebald, and D. Guyomar, J. Cryst. Growth **275**, 580 (2005).
[17]S. Priya and K. Uchino, J. Appl. Phys. **91**, 4515 (2002).
[18]S. Zhang, L. Lebrun, C. A. Randall, and T. R. Shrout, Phys. Status Solidi A **202**, 151 (2005).
[19]X. Ren and K. Otsuka, Nature (London) **389**, 579 (1997).
[20]X. Ren and K. Otsuka, Phys. Rev. Lett. **85**, 1016 (2000).
[21]L. X. Zhang, W. Chen, and X. Ren, Appl. Phys. Lett. **85**, 5658 (2004).
[22]A.-E. Renault, H. Dammak, G. Cabvarin, M. Pham Thi, and P. Gauchrer, Jpn. J. Appl. Phys., Part 1 **41**, 3846 (2002).
[23]S. J. Zhang, L. Lebrum, S. Rhee, R. E. Eitel, C. A. Randall, and T. R. Shrout, J. Cryst. Growth **210**, 236 (2002).
[24]IEEE, ANSI/IEEE Standard No. 176–1987.
[25]A.-E. Renault, H. Dammak, P. Gaucher, M. Pham Thi, and G. Calvarin, Proceedings of the 13th IEEE ISAF, 2002, pp. 439–442.
[26]M. Guennou, H. Dammak, and M. P. Thi, J. Appl. Phys. **104**, 074102 (2008).
[27]K. Carl and K. H. Härdtl, Ferroelectrics **17**, 473 (1978).
[28]L. Zhang and X. Ren, Phys. Rev. B **73**, 094121 (2006).
[29]D. Kobor, Ph.D. thesis, INSA Lyon (2005).
[30]W. L. Warren, G. E. Pike, K. Vanheusden, D. Dimos, B. A. Tuttle, and J. Robertson, J. Appl. Phys. **79**, 9250 (1996).
[31]U. Robels and G. Arlt, J. Appl. Phys. **73**, 3454 (1993).
[32]R.-A. Eichel, P. Erhart, P. Traskelin, K. Albe, H. Kungl, and M. J. Hoffmann, Phys. Rev. Lett. **100**, 095504 (2008).
[33]H. Mestric, R.-A. Eichel, T. Kloss, K.-P. Dinse, So. Laubach, St. Laubach, and P. C. Schmidt, Phys. Rev. B **71**, 134109 (2005).
[34]D. Damjanovic, M. Budimir, M. Davis, and N. Setter, J. Mater. Sci. **41**, 65 (2006).
[35]M. Davis, M. Budimir, D. Damjanovic, and N. Setter, J. Appl. Phys. **101**, 054112 (2007).